Int. J. Electrochem. Sci., 7 **(2012)** 9859 - 9868

International Journal of
ELECTROCHEMICAL
SCIENCE
www.electrochemsci.org

Kinetics and Electrochemical Studies of Fe-substituted $LiMnPO_4$

Jiali Liu, Xiaoyu Liu, Tao Huang, Aishui Yu[*]

(Department of Chemistry and Shanghai Key Laboratory of Molecular Catalysis and Innovative Materials, Institute of New Energy, Fudan University, 2205 Songhu Road, Shanghai 200433, China)
[*]E-mail: asyu@fudan.edu.cn

Received: 30 July 2012 / *Accepted:* 29 August 2012 / *Published:* 1 October 2012

A simple sol-gel method was applied to synthesize $LiMn_{(1-x)}Fe_xPO_4$ (x=0-0.5). The kinetics of $LiMn_{(1-x)}Fe_xPO_4$ was studied by chemical delithiation experiment and EIS measurements. The results showed that the $LiMn_{0.6}Fe_{0.4}PO_4$ has the fastest conversion rate from $LiMn_{(1-x)}Fe_xPO_4$ to $Mn_{(1-x)}Fe_xPO_4$ which might be related to the best rate capability among all these samples. The electrochemical tests showed that the discharge capacity for it is about 130 $mAhg^{-1}$, 100 $mAhg^{-1}$, 80 $mAhg^{-1}$and 60 $mAhg^{-1}$ at 0.1 C, 0.5 C, 1 C, and 2 C respectively.

Keywords: chemical delithiation; $LiMnPO_4$/C; lithium ion battery; discharge capacity; rate capability

1. INTRODUCTION

Lithium transition-metal phosphate $LiMPO_4$ (M=Mn, Fe, Co, Ni) has attracted broad attention as potential Li-ion battery cathode material due to their advantages of lower cost, higher electrochemical and thermal stabilities [1-3]. So they are believed to be the most promising candidates as the cathode materials for large-scale lithium-ion batteries [4-6]. Ascribed to the strong covalent bonds between oxygen ions and the P^{5+} in PO_4^{3-} tetrahedral polyanions, these olivine structural compounds have stable three-dimensional framework which ensure the higher stability without structural re-arrangement during lithiation and de-lithation [7-10].

Lithium manganese phosphate ($LiMnPO_4$) is of great interest due to its higher redox voltage of 4.1 V plateau for Mn^{2+}/Mn^{3+} versus Li^+/Li [11-13]. Moreover, the theoretical energy density is also 1.2 times greater than that of $LiFePO_4$ [14-16]. However, due to its intrinsic low electronic and ionic conductivity, its current effective energy density is much smaller compared [17, 18]. This serious drawback of slow kinetics leads to the poor discharge capacity and rate capability for $LiMnPO_4$. Up to

now, several previous literatures have shown that partial substitution of Mn by Fe in the olivine structure could successfully improve the kinetics. Padhi first mentioned that only $Li[Mn_xFe_{1-x}]PO_4$ ($x < 0.75$) would be electrochemically active [1]. Molenda revealed that the electronic conductivity of $LiFe_{0.45}Mn_{0.55}PO_4$ is one order magnitude higher than undoped $LiFePO_4$ [20]. B. Scrosati synthesized micrometer-sized, spherical $LiMn_{0.85}Fe_{0.15}PO_4$ to assuring high tap density [21]. Y. K. Sun explored the co-precipitation method to synthesize $Mn_{0.5}Fe_{0.5}PO_4$ precursor, and the as-prepared $LiMn_{0.5}Fe_{0.5}PO_4$/C composite delivered excellent electrochemical performance [22]. The group of D. Aurbach prepared nano-sized $LiMn_{0.8}Fe_{0.2}PO_4$/C with conventional solid-state method, and the discharge capacity of this material was 160 $mAhg^{-1}$ [23]. K. Saravanan prepared $Li[Mn_xFe_{1-x}]PO_4$ ($x = 0.5, 0.75,1$) by simple solvothermal method and $LiMn_{0.5}Fe_{0.5}PO_4$ nanoplate exhibited the best electrochemical performance [23]. However, the optimized amounts of Fe doping as the increase of kinetics has not been established.

In this paper, a series of experiments including chemical delithiation and EIS measurements were carried out on $LiMn_{(1-x)}Fe_xPO_4$(x=0-0.5) composites to analyze its lithium diffusion kinetics. It is proved that the amount of Fe is crucial to lithium diffusion kinetics in Mn based olivine structured $LiMPO_4$.

2. EXPERIMENTAL

2.1 Synthesis of materials

$LiMn_{(1-x)}Fe_xPO_4$(x=0-0.5) powder was synthesized by a sol-gel method as previous [24]. The starting material of manganese acetate tetrahydrate ($Mn(CH_3COO)_2{\cdot}4H_2O$, Sinopharm Chemical Reagent Co. Ltd., Shanghai, AR), ferric nitrate ($FeNO_3$, Sinopharm Chemical Reagent Co. Ltd., Shanghai, AR), ammonium dihydrogen phosphate ($NH_4H_2PO_4$, Sinopharm Chemical Reagent Co. Ltd., Shanghai, AR) and citric acid monohydrate (Sinopharm Chemical Reagent Co. Ltd., Shanghai, AR) were dissolved in deionized water at room temperature with a molar ratio of 1-x : x : 1 :1 (x = 0-0.5) . Then under magnetic stirring, the stoichiometric amounts of lithium acetate dehydrate ($LiAc{\cdot}2H_2O$, Sinopharm Chemical Reagent Co. Ltd., Shanghai, AR) solution was added. Homogeneous gels were obtained under rigorous stirring at 80 °C. After the gels were dried at 120 °C overnight, the resulting powder was initially heated at 350 °C for 3 h in Ar containing 5% H_2. After being cooled down to room temperature, the products were milled again for about 1 h, and then calcined at 550°C for 5 h in the same atmosphere.

2.2 Chemical Delithiation

The chemically delithiated process was conducted according to the previous studies [25]. The $LiMn_{1-x}Fe_xPO_4$ (x=0-0.5) and NO_2BF_4 (Nitronium tetrafluoroborate) (Aldrich) were stirred in acetonitrile at room temperature in an Argon-filled glovebox for about 10 h. NO_2BF_4 is a strong

oxidizing agent with a high redox potential of NO^{2+}/NO_2 at 5.1 V VS Li^+/Li. Hence, the reaction was as follows:

$$LiMnPO_4 + NO_2BF_4 = y\ MnPO_4 + LiBF_4 + NO_2 + (1\text{-}y)\ LiMnPO_4$$

2.3 Characterization

The X-ray diffraction (XRD) measurement was carried out on a Bruker D8 Advance X-ray diffraction using Cu Kα radiation source (λ=1.5406 Å) with a step size of 4 ° min^{-1} from 10 to 80 °. The powder morphology was observed by scanning electron microscope (SEM) on JEOL JSM-6390. The Li, Fe, P contents of the samples were analyzed by inductively coupled plasma (ICP, Thermo E.IRISDuo) and atomic absorption spectroscopy (AAS) (Z-5000).

2.4 Electrochemical measurements

The electrochemical performance of as-prepared $LiMnPO_4$ was investigated by using coin cells assembled in an argon-filled glove box (SIMATIC OP7, MBRAUN). The cell was composed of a lithium anode and a cathode that was a mixture of prepared $LiMnPO_4$ (70%), Super P Carbon black (20%) and polytetrafluoroethylene (PTFE) (Dupont) (10%). The mixture was rolled into a thin sheet with uniform thickness, then it was cut into 10×10 mm section before being pressed to a aluminum mesh. Typical loading of the active material is about 10 mg cm^{-2}. The electrolyte was 1 M $LiPF_6$ dissolved in a mixed solvent of ethylene carbonate (EC) and dimethyl carbonate (DMC) (1:1 in weight), and Celgard 2300 was used as separator. The electrochemical analysis instrument (EIS) measurements were performed on a CHI660 B electrochemical analysis instrument. Charge-discharge performance was conducted on LAND CT 2001 cell test instrument (Wuhan Kingnuo Electronic Co, China). All the tests were performed at room temperature.

3. RESULTS AND DISCUSSION

3.1 Material identification

The diffraction patterns of as-prepared $LiMn_{1-x}Fe_xPO_4$ (x=0-0.5) composites were shown in Fig. 1 a). It can be seen that all the powders have a well ordered olivine structure with the space group of orthorhombic Pnma. There were no any impurities could be found from the XRD data and the sharp peaks also indicated the high crystallization. Fig. 1 b) magnified the peaks of (200) plane for unsubstituted and substituted samples (x=0, 0.2, 0.4). The peaks shifted continuously toward higher angel which indicated the Fe^{2+} successfully entered the crystal lattice. SEM photos revealed the similar morphology for these samples and the particle size were all about 300-350nm.

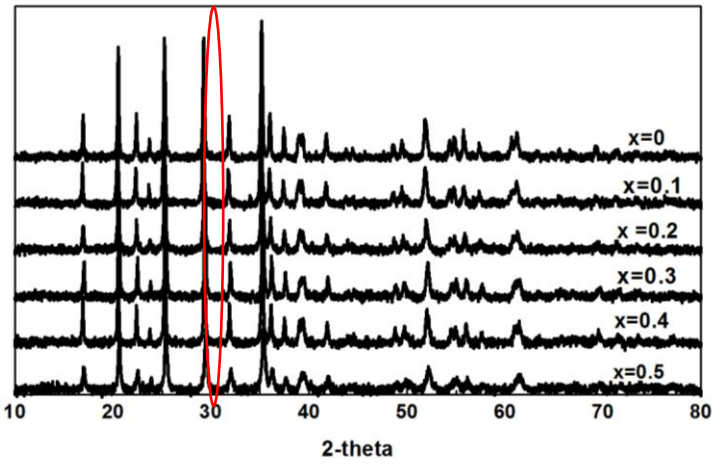

A

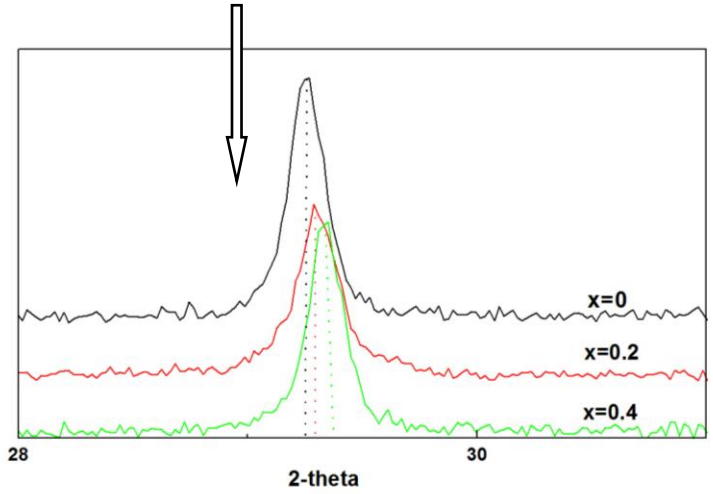

B

Figure 1. a) XRD data of the samples $LiMn_{(1-x)}Fe_xPO_4$ (x=0-0.5), b) XRD data for some substitute

3.2 Chemical Delithiation

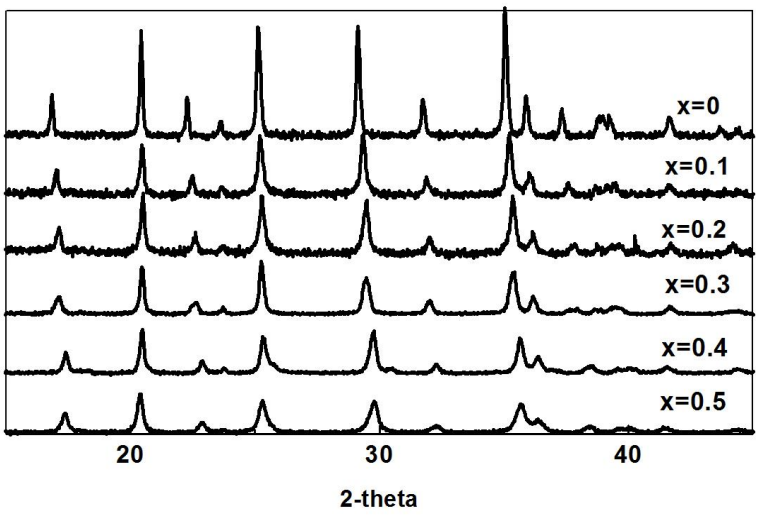

A

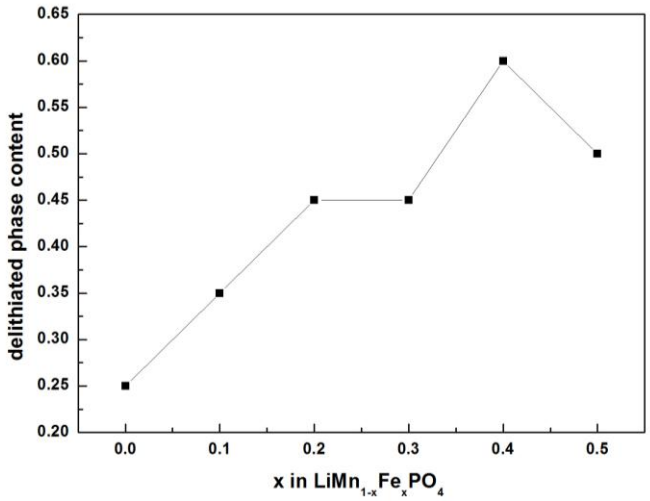

B

Figure 2. a) XRD data of the samples after treated with 100% NO_2BF_4, b) the delithiated phase content of the samples after treated with 100% NO_2BF_4

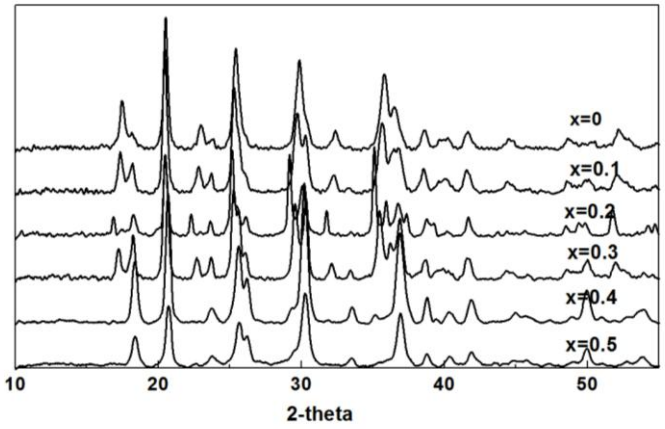

A

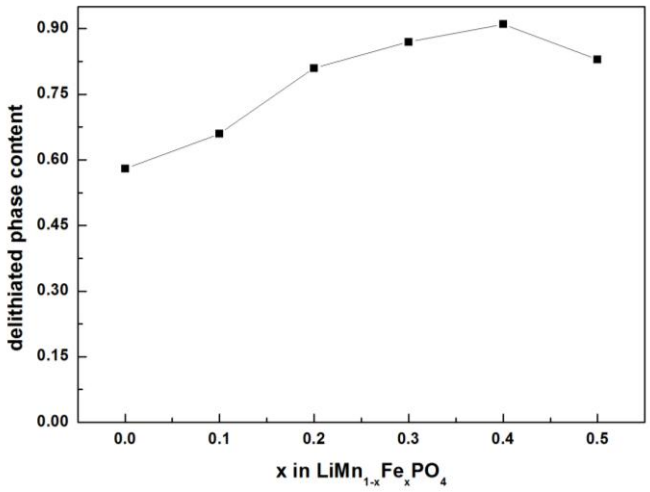

B

Figure 3. a) XRD data of the samples after treated with 200% NO_2BF_4, b) the delithiated phase content of the samples after treated with 200% NO_2BF_4

All the previous studies have shown that amount of Fe substitution would influence the electrochemical behavior for the sample. Hence, to study the kinetics of all the samples, chemical delithiation and EIS measurements were both used. Fig.2 showed the XRD data of obtained samples which were delithiated with 100% mol NO_2BF_4 in ancetonitrile. It can be seen that the diffraction pattern for all the samples were still olivine structure. Besides, the pattern of $LiMn_{0.6}Fe_{0.4}PO_4$ shows the second phase of $Mn_{0.6}Fe_{0.4}PO_4$ which was labeled by asterisk. There were previous literatures showed that solid solution of Li_yMnPO_4 would be formed during chemical and electrochemical delithiation process. The conversion rate which is defined as the ratio between the delithiated and the lithiated phase can be used as a measure for the kinetics performance of phosphate material. This conversion rate could be obtained by analysis the lithium content in ancetonitrile. Fig.2 b summarized the delithiated phase content for the samples which decided by the lithium content in ancetonitrile after reaction. Due to intrinsic low conductivity, the unsubstituted $LiMnPO_4$ only reached 25% oxidation with 100% NO_2BF_4. However, all the Fe substituted materials showed improved kinetics, as suggested by the lithium content in ancetonitrile. It was worth mentioning that the sample with x=0.4 had the highest delithiated phase content which was consistent with the XRD data.

It is believed that the conversion rate also related to the amount of NO_2BF_4 in the delithiation process. With 200% NO_2BF_4, all the samples showed the second phase which suggested by the XRD data (Fig.3 a). It was understandable that the conversion rate increased with increasing NO_2BF_4 content. The diffraction peak for the second phase of $Mn_{1-x}Fe_xPO_4$ became more obvious from $LiMnPO_4$ to $LiMn_{0.7}Fe_{0.3}PO_4$. Moreover, for samples of $LiMn_{0.6}Fe_{0.4}PO_4$ and $LiMn_{0.5}Fe_{0.5}PO_4$ were both converted to single delithiated phases. The conversion rates which decided by the lithium content in ancetonitrile were displayed in Fig. 3 b. It could be seen that 90% oxidation was reached for $LiMn_{0.6}Fe_{0.4}PO_4$ here. Hence, among these electrodes, $LiMn_{0.6}Fe_{0.4}PO_4$ delivered the highest lithium delithiated rate.

3.3 Electrochemical Behaviour

In aim of further revealing the lithium diffusion kinetics in the samples, the subsequent electrochemical impedance (EIS) measurements were carried out in the frequency range from 10 mHz to 100 kHz at the open circuit with an ac voltage signal of 5 mv. All the Nyquist plots exhibited in Fig. 4 a are composed of a semicircle in the high frequency region and a line in the low frequency region. The semicircle was ascribed to the charge transfer resistance between the electrolyte and the active material. It is obvious that unsubstituted $LiMnPO_4$ delivered the largest resistance and that of $LiMn_{0.6}Fe_{0.4}PO_4$ showed the smallest.

The straight line was related to the lithium diffusion process. The plots of Z_{re} against $\omega^{-1/2}$ were depicted in Figure 6 b), it corresponding to the Equation (2), and σ is the slope of the straight line.

$$Z^{"} = \sigma\omega^{-1/2}$$

$$D = \frac{R^2T^2}{2A^2n^4F^4C^2\sigma^2}$$

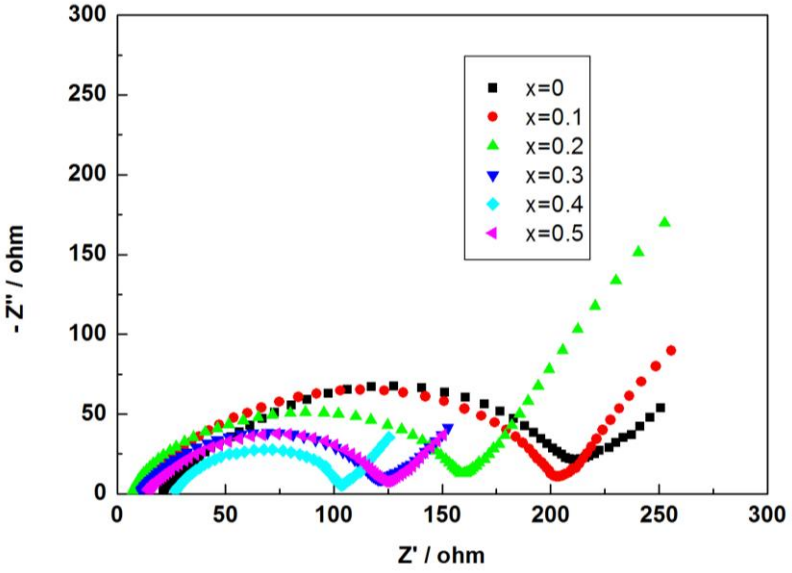

A

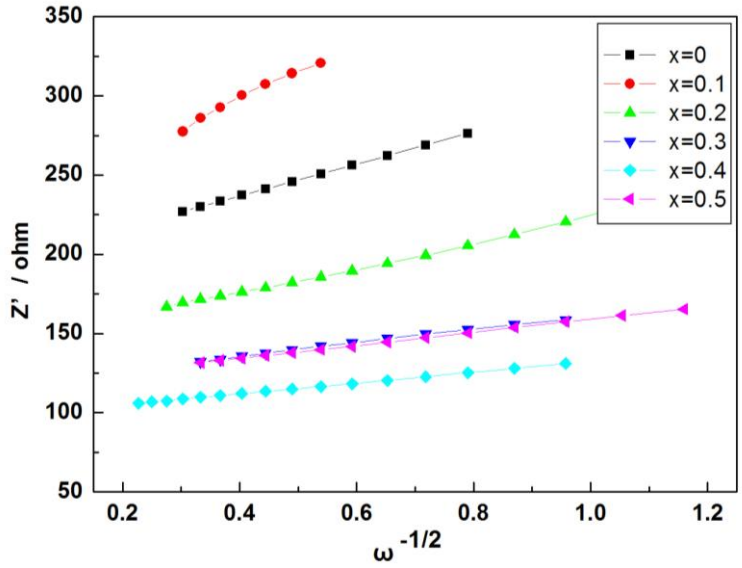

B

Figure 4. a) Electrochemical impedance spectra characterization of the samples at open circuit; b) Graph of Z' plotted against $\omega^{-1/2}$

Where R is the gas constant, T is the room absolute temperature in our experiment, A is the surface area of the electrode, n is the number of electrons per molecule attending the electronic transfer reaction, F is Faraday constant, C is the concentration of lithium ion in $LiFePO_4$ electrode, respectively.

With calculation, we obtained the lithium diffusion constant $\tilde{D}$ ($cm^2\ S^{-1}$) in electrodes of these samples. Be consistent with the XRD data, $LiMnPO_4$ showed the smallest one of $9.71\times10^{-14}\ cm^2\ S^{-1}$. It is clear that the lithium ion diffusion coefficient decreases with increasing Fe substitution and $LiMn_{0.6}Fe_{0.4}PO_4$ delivered the largest value of $8.5\times10^{-13}\ cm^2\ S^{-1}$. Hence, the result obtained by EIS was consistent with the chemical delithiation process.

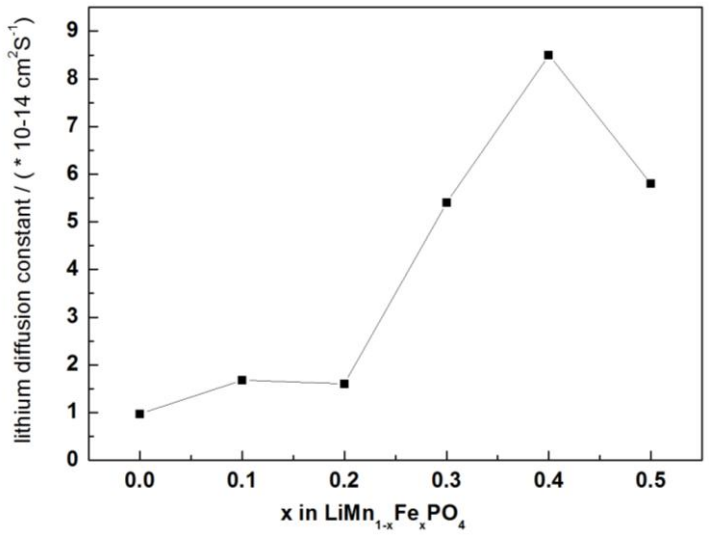

Figure 5. the lithium diffusion constant for the samples

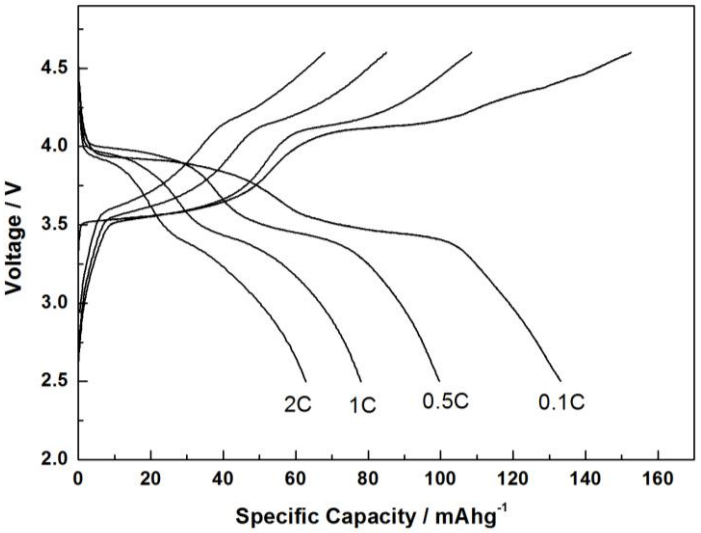

Figure 6. the charge-discharge curves of $LiMn_{0.6}Fe_{0.4}PO_4$ at different rate

Although there're several reports on the improved electrochemical behavior of $LiFe_{1-x}Mn_xPO_4$ compared to LiMnPO4, the kinetics was discussed little. J. Molenda analyzed the electrical conductivity and reaction with lithium of $LiFe_{1-y}Mn_yPO_4$ olivine type cathode materials [28]. It was revealed that the electronic conductivity of $LiFe_{0.45}Mn_{0.55}PO_4$ was distinctly higher as compared with $LiFePO_4$ and $LiMnPO_4$. M. W. Li suggested that the electrochemical behavior could be improved by Fe substation and $LiFe_{0.25}Mn_{0.75}PO_4$ exhibits the longest charge-discharge voltage [29]. In this paper, we analyzed the lithium diffusion kinetics of $LiFe_{1-y}Mn_yPO_4$ (x=0-0.5), and the sample of x=0.4 showed the highest lithium diffusion constant. Maybe this could be ascribed to the lower activation energy for it.

Fig.6 displayed the charge-discharge plots for $LiMn_{0.6}Fe_{0.4}PO_4$ at different rate. There were two obvious plateau in these curves which could be ascribed to Mn^{2+}/Mn^{3+} and Fe^{2+}/Fe^{3+} two phase reaction. The discharge capacity was about 130 $mAhg^{-1}$, 100 $mAhg^{-1}$, 80 $mAhg^{-1}$ and 60 $mAhg^{-1}$ at 0.1 C, 0.5 C, 1 C, and 2 C respectively. And the rate capability was displayed in Fig. 7. The electrochemical performance was not excellent compared to some previous literatures. Although 40% amount of Fe substitution could improve the electronic and ionic conductivity for this $LiMnPO_4$ here. The size of 200-300 nm is still a disadvantage for it to elaborate its potential. Reduction of the particles to less than 100 nm size dimension is an effective way for reduction of lithium path way and increase of the contact area with electrolyte. Hence, our further work will be focused on improve the electrochemical performance of $LiMn_{0.6}Fe_{0.4}PO_4$ material by optimizing the method to realize the reduction of particle size.

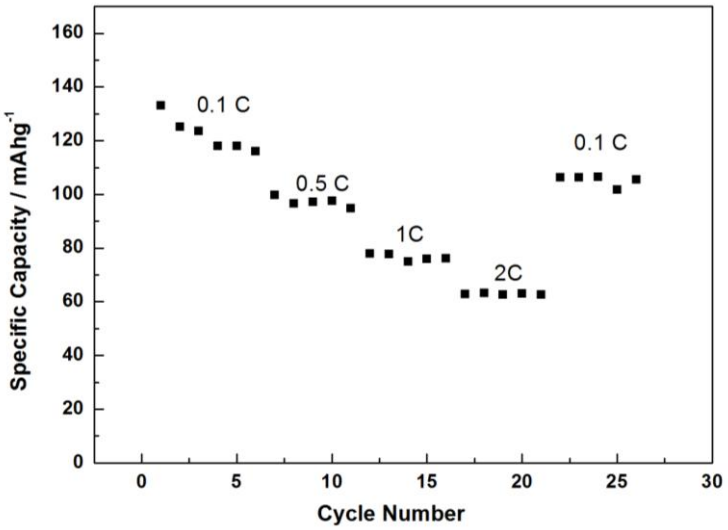

Figure 7. the rate capability of $LiMn_{0.6}Fe_{0.4}PO_4$

4. CONCLUSION

The kinetics of $LiMn_{(1-x)}Fe_xPO_4$ (x=0-0.5) synthesized by sol-gel method was compared. The conversion rate which obtained by analysis of lithium content in ancetonitrile after chemical delithiation process was employed as a measure for the kinetics performance of all the samples. After treatment with 100% NO_2BF_4 oxidant in the experiment, only $LiMn_{0.6}Fe_{0.4}PO_4$ showed the second phase of $Mn_{0.6}Fe_{0.4}PO_4$ in the XRD data while the largest amount of delithiated phase for 200% NO_2BF_4 oxidant. The EIS measurements also revealed the result that $LiMn_{0.6}Fe_{0.4}PO_4$ showed the largest kinetic among the samples.

References

1. A.K. Padhi, K.S. Nanjundaswamy, J.B. Goodenough, *J. Electrochem. Soc.* 144

(1997) 1188.
2. M.S. Islam, D.J. Driscoll, C.A.J. Fisher, P.R. Slater, *Chem. Mater*. 17 (2005) 5085.
3. B. Kang, G. Ceder, *Nature* 458 (2009) 190.
4. Y.-N. Xu, W.Y. Ching, Y.-M. Chiang, *J. Appl. Phys*. 95 (2004) 6583 e 6585.
5. C.A.J. Fisher, V.M.H. Prieto, M.S. Islam, *Chem. Mater*. 20 (2008) 5907e5915..
6. M. Higuchi, K. Katayama, Y. Azuma, M. Yukawa, M. Suhara, *J. Power Sources*, 119 (2003) 258-261.
7. S. K. Martha, B. Markovsky, J. Grinblat, Y. Gofer, O. Haik, E. Zinigrad, D. Aurbach, T. Drezen, D. Wang, G. Deghenghi, I. Exnar, *J. Electrochem. Soc*., 156 (7) (2009) A541-A552.
8. T. Drezen, N. H. Kwon, P. Bowen, I. Teerlinck, M. Isono, I. Exnar, *J. Power Sources*, 174 (2007) 949-953.
9. C.A.J.Fisher, V.M.H.Prieto, M.S.Islam, *Chem. Mater*., 20 (2008) 5907-5915.
10. H. H. Chang, C. C. Chang, H. C. Wu, Z. Z. Guo, M. H. Yang, Y. P. Chiang, H. S. Sheu, N. L. Wu, *J. Power Sources*, 158 (2006) 550-556
11. A. Eftekhari, *J. Electrochem. Soc*., 151 (2004) A1816-A1819.
12. C. Delacourt, P. Poizot, M. Morcrette, J. M. Tarascon and C. Masquelier, *Chem. Mater*. , 2004, 16, 93–99.
13. B. Ellis, P. S. Herle, Y. H. Rho, L. F. Nazar, R. Dunlap, L. K. Perry, D. H. Ryan, Faraday Discuss., 2007, 134, 119–141.A390-A395.
14. C. Delacourt, L. Laffont, R. Bouchet, C. Wurn, J. B. Leriche, M. Morcrette, J. M. Tarascon, C. Masquelier, *J. Electrochem. Soc.*, 152 (2005) A913.
15. S. Y. Chung, J. T. Bloking, *Nat. Mater*., 2 (2002) 123.
16. G. Li, H. Azuma, M. Tohoda, *Electrochem. Solid-State Lett*.,5 (2002) A135.
17. J. Molenda, W. Qjczyk, J. Marzec, *J. Power Sources*, 174 (2007) 689.
18. Y. K. Sun, S. M. Oh, H. K. Park, B. Scrosati, *Adv. Mater.*, 23 (2011) 5050.
19. K. Saravanan, V. Ramar, P. Balaya, J. J. Vittal, *J. Mater. Chem*., 21(2011) 14925.
20. C. M. Burba, R. French, *J. Electrochem. Soc*., 151 (2004) A1032.
21. Y. K. Sun, S. M. Oh, H. K. Park, B. Scrosati, *Adv. Mater*., 23 (2011) 5050.
22. S. M. Oh, S. T. Myung, Y. S. Choi, K. H. Oh, Y. K. Sun, *J. Mater. Chem*., 21 (2011) 19368.
23. S. K. Martha, J. Grinblat, O. Haik, E. Zinigrad, T. Drezen, J. H. Miners, I. Exnar, A. Kay, B. Markovsky, D. Aurbach, *Angew. Chem*., 121 (2009) 8711.
24. J. K. Kim, G. S. Chauhan, J. H. Ahn, H. J. Ahn, *J. Power sources*, 189 (2009) 391.
25. C. Delacourt, L. Laffont, R. Bouchet, C. Wurm, J. B. Leriche, M. Morcrette, J. M. Tarascon, C. Masquelier, *J. Electrochem. Soc*., 152(5) (2005) A913.
28. J. Molenda, W. Ojczyk, J. Marzec, *J. Power Sources*, 174 (2007) 689.
29. L. Chen, Y. Q. Yuan, X. Feng, M. W. Li, *J. Power Sources*, 214 (2012) 344.